

14. Marshall, G. J., *Int. J. Climatol.*, 2006, **27**, doi:10.1002/joc.1407.
15. Solomon, S., Portmann, R. W. and Thompson, D. W. J., *Proc. Natl. Acad. Sci. USA*, 2007, **104**, 445–449.
16. Kerr, R. A., *Science*, 2002, **296**, 825–826.
17. Thompson, D. W. J. and Solomon, S., *Science*, 2002, **296**, 895–899.

ACKNOWLEDGEMENTS: I thank the anonymous reviewers for their valuable comments; J. D. Shanklin, Natural Environment Research Council–British Antarctic Survey (<http://www.antarctica.ac.uk/met/jds/ozone/#>

data), for providing the total ozone data for Halley and Vernadsky stations; Scripps Institution of Oceanography, Scripps CO<sub>2</sub> Program (<http://scrippsco2.ucsd.edu/>) for providing the atmospheric CO<sub>2</sub> concentrations in the south pole; Carbon Dioxide Information Analysis Center, Oak Ridge National Laboratory, US Department of Energy, Tennessee (<http://www.antarctica.ac.uk/met/gjma/>) for providing surface temperature for 18 stations distributed over the entire Antarctic continent over a period of five decades and Prof. J. N. Goswami, Director, Physical Research Laboratory, Ahmedabad for providing library facility. Figure 6 representing the multivariate ENSO index has been taken from the website:

<http://www.esrl.noaa.gov/psd/enso/mei/index.html>. The sunspot numbers have been downloaded from the website: <http://solarscience.msfc.nasa.gov/SunspotCycle.shtml>.

Received 20 November 2012; revised accepted 8 May 2013

NANDITA D. GANGULY

*Department of Physics,  
St Xavier's College,  
Ahmedabad 380 009, India  
e-mail: ganguly.nandita@gmail.com*

## Remote sensing of moving objects

Traditionally, moving object characterization with remote sensors was done using RADAR systems, image sequences or videos<sup>1,2</sup>, but, it is not always possible to acquire these datasets. However, recent developments in very high resolution (VHR) remote sensing sensors have opened a new opportunity in extracting moving object information using single-pass optical imagery. For this type of application, the challenges include: first, extracting target location in both multispectral (MS) and panchromatic (PAN) bands and second, exploiting the small time lag between the acquisition of MS and PAN bands created due to typical construction of line scanners. Several researchers have attempted to identify and estimate velocity of moving targets using single VHR optical images, for example, using 1 m resolution satellite and airborne images<sup>3</sup>, Quickbird images<sup>4,5</sup> or IKONOS images<sup>6</sup>. Extraction of the target location becomes difficult with decreasing spatial resolution. The spatial resolution of MS bands in Quickbird and IKONOS is 2.4 and 4 m respectively, which is comparable with the dimension of small/medium (length less than 4 m) vehicles and is insufficient for inferring the shape of larger vehicles. Fusion of MS and PAN bands is not a solution in such cases because of the apparent mismatch in these bands for moving objects. This issue can be successfully addressed using finer resolution MS and PAN images having a finite time gap between acquisitions.

WorldView2 (WV2), launched in October 2009, provides 2 m spatial resolution,

8-band MS images and 0.5 m resolution PAN images, which is the highest spatial resolution among all commercially available satellites at present. Few studies have used single-pass WV2 images for moving target information extraction<sup>7,8</sup>. In this study, the potential of WV2 images for identifying and characterizing moving targets has been explored. Eight MS bands of WV2 system are arranged in two arrays (MS1 and MS2) of four MS bands each: MS1 consists of NIR1, Red, Green and Blue, and MS2 consists of Red Edge, Yellow, Coastal and NIR2. The focal plane layout of WV2 is shown in Figure 1.

The MS arrays are positioned on either side of the PAN array. Due to this hardware arrangement, the sequence of image collection in MS1, PAN and MS2 leads to a time lag of approximately 0.17 s

between PAN and MS1/2 and 0.35 s between MS1 and MS2 (ref. 7). Besides this, hardware limitations have put further constraints on the Time Delay and Integration (TDI) settings of the MS bands: the following pairs, i.e. NIR1 and Red; Green and Blue; Red Edge and Yellow, and Coastal and NIR2 must have the same TDI (ref. 9), creating maximum time lag between NIR1 and NIR2 acquisition.

In most cases, inter-band time lag is not negligible for movement detection. However, for fast-moving objects like aircraft, due to this time lag a displacement is caused between object positions when viewed in different bands. Therefore, an aircraft visible in WV2 image, acquired on 19 February 2010 was selected as a moving object. The object in eight different bands is shown in

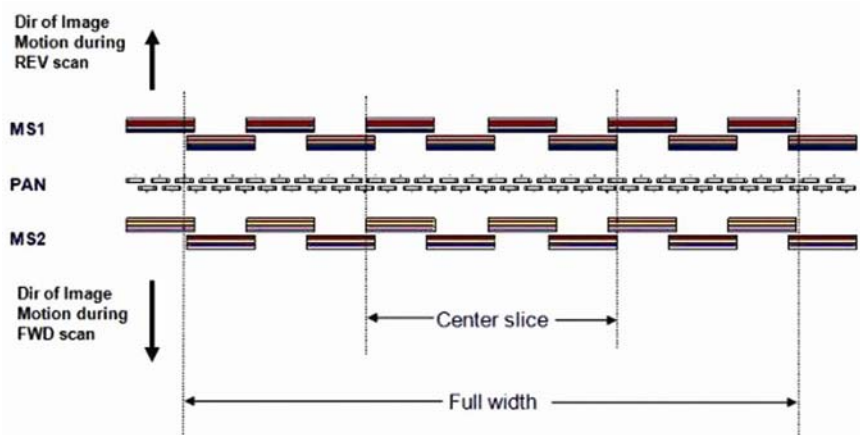
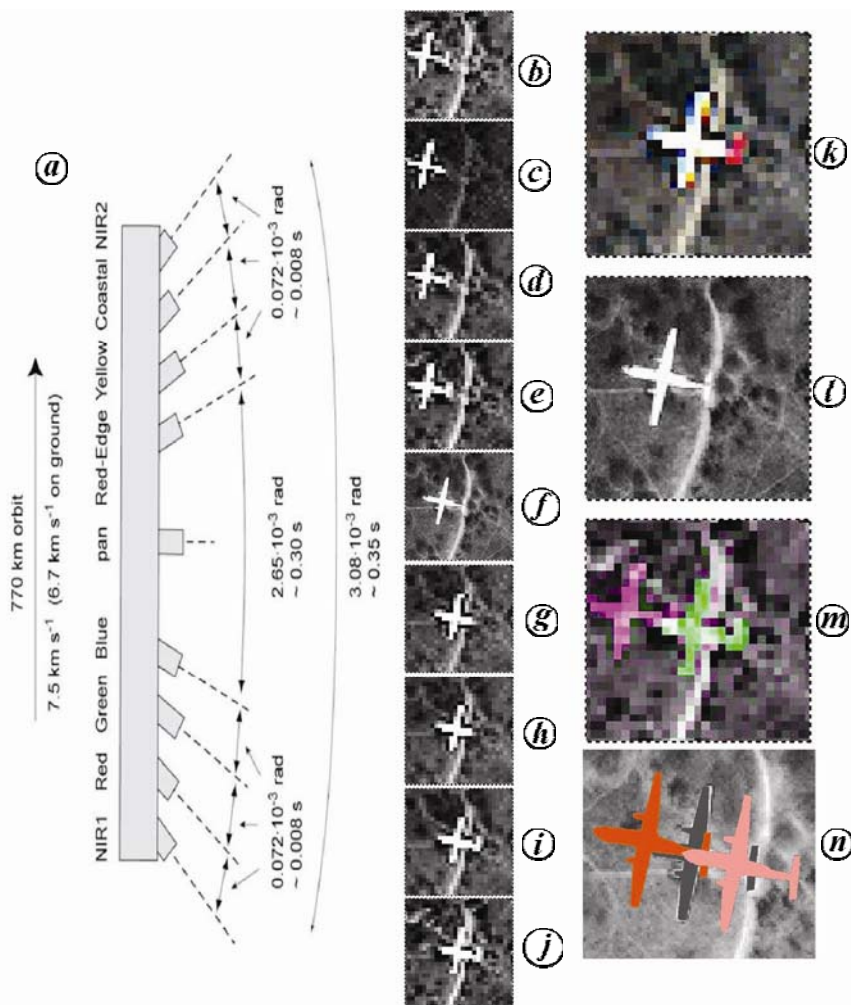


Figure 1. The focal plane layout of WorldView2 (source: DigitalGlobe<sup>9</sup>).



**Figure 2.** *a*, Structure of WV2 focal plane showing angular differences between the optical axes and corresponding time lags between the MS and PAN sensors (source: ref. 7). *b–j*, Images of the aircraft in NIR2, Coastal, Yellow, Red Edge, PAN, Blue, Green, Red and NIR1 respectively. *k–m*, Aircraft in true colour composite, PAN and NIR2–NIR1 bands. *n*, Delineation of aircraft using NIR2–PAN–NIR1 bands.

Figure 2 *b–j*. The true colour composite image is shown in Figure 2 *k*. There is a colour shift along the direction of movement: the head appears cyan and tail appears red. Initially, an attempt was made to identify the aircraft model by measuring its physical dimensions in PAN band and finding a match with existing database. The position and shape of the aircraft was manually digitized over the PAN imagery. It was found that the mean length and wing span are 24 (with standard deviation of 2.3 m) and 27 m (with standard deviation of 0.8 m) respectively. This is a single-turbine aircraft, operating in short to medium range. The nearest match is ATR 72-500 with wingspan 27.05 m, length 27.17 m and having a single turbine (Figure 3 *a*). The underestimation in length is due to the presence of bright features in the rear region of the aircraft in PAN band, which partially camouflages the exact horizontal tail position (Figure 3 *b*). This aircraft is listed under Directorate General of Civil Aviation (DGCA) aircraft type statistics<sup>10</sup>. In 2010, Kingfisher and Jet Airways regularly operated this aircraft.

Due to different image capturing sequences of MS1, MS2 and PAN, the aircraft appears at three positions in a single image and the distances between these are directly proportional to the velocity. Therefore, for calculating speed of the aircraft, three time-lag conditions were considered: between MS1 and PAN ( $\Delta t_{PAN-MS1}$ ), MS2 and PAN ( $\Delta t_{PAN-MS2}$ ) and MS1 and MS2 ( $\Delta t_{MS1-MS2}$ ). The corresponding distances ( $\Delta d_{PAN-MS1}$ ,  $\Delta d_{PAN-MS2}$  and  $\Delta d_{MS1-MS2}$ ) travelled by the target was calculated from the image. The position and shape of the aircraft interpreted from the satellite was placed over its respective positions in MS1 and MS2 images. The positional error was minimized in the process. Multiple match points (which could be easily identified, such as corner location, head and turbine position, etc.) were considered to reduce the effect of target localization and change in orientation. The position shift for different bands was manually determined for the multiple match points using the image shown in Figure 2 *n*. Speed (in m/s) was estimated using  $v (= \Delta d / \Delta t)$ . Various distances calculated using different match points and speed estimate are given in Table 1.

From Figure 2 *a*, it is evident that NIR1 and NIR2 have maximum time lag

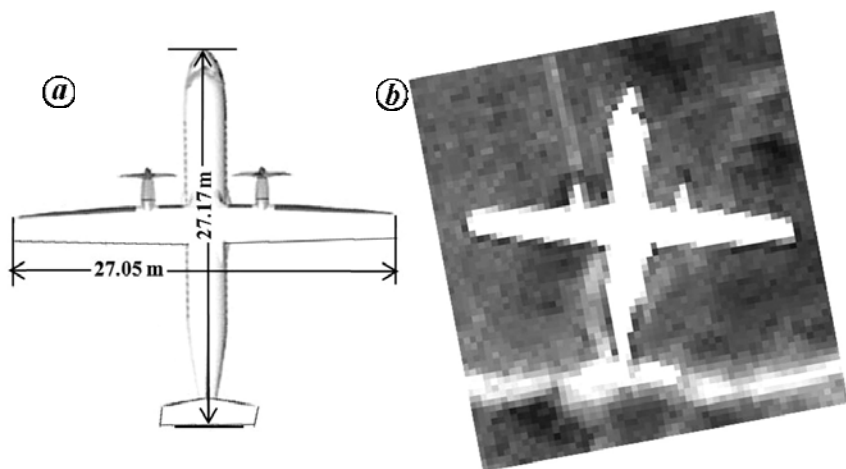


**Figure 3.** *(a)* Schematic top view of ATR 72-500 (source: ref. 12) along with dimensions. This matches with the PAN image of the aircraft shown in *(b)* with respect to overall external structure, turbine number and position, wing span and body length ratio.

**Table 1.** Details of distance between match points (calculated from Figure 2n)

Match points	$\Delta d_{PAN-MS2}$ (m)	$\Delta d_{PAN-MS1}$ (m)	$\Delta d_{MS1-MS1}$ (m)	
1	9.45	7.98	17.47	Estimated speed (m/s): 49.91 with standard deviation of 3.22
2	9.39	8.12	17.47	
3	9.35	8.14	17.46	
4	9.29	8.18	17.48	
5	9.25	8.22	17.45	
6	9.27	8.21	17.45	
7	9.09	8.35	17.45	

of 0.35 s. Therefore, NIR1 and NIR2 were taken as representatives from the corresponding MS groups. The aircraft was found to be flying at an average speed of 49.91 m/s ( $\pm 3.22$  m/s). The position of the plane was about 2000 m away from the runway. According to reports<sup>11,12</sup>, the landing speed of ATR 72-500 is 115 KIAS ( $\sim 59$  m/s). The difference between the calculated and expected speed is less than 9 m/s. This can be caused by target localization error in MS bands by single pixel (2 m).

This study shows the potential of VHR single-pass optical images for moving object identification and speed estimation. In particular, the study demonstrates application of VHR remote sensing instruments for speed and direction estimation of moving objects. Considering the available database, the identified object and estimated speed are found to be plausible and consistent. Fully automatic detection of object is required over visual inspection. More accurate identification of objects can result in better estimation of speed. Future work will focus on using Rational Polynomial Coefficient (RPC) of the sensor to transform the image space to ground space. Further efforts can be of great value to understand effects of object movement on image fusion. This would also need research in object-based extraction and

image segmentation. These possibilities also open perspectives for research in traffic and vehicle movement management. High growth in road traffic volume is among the important issues of urbanization in developing nations. Understanding and tapping information on vivid traffic situations and moving information computation can imbibe real-time scenarios in animation science. With the aid of the concept presented in this study, the detection of vehicle (both surface and airborne) can be automated<sup>4,8</sup>. This automation will contribute in situations related to natural disaster<sup>13</sup> and surveillance (homeland and border security), where emergency response is of immediate importance.

1. Munno, C. J., Turk, H., Wayman, J. L., Libert, J. M. and Tsao, T. J., In Security Technology Proceedings, Institute of Electrical and Electronics Engineers, International Carnahan Conference, 13–15 October 1993, pp. 47–57.
2. Nag, S. and Barnes, M., In Proceedings of the IEEE Radar Conference, Huntsville, Alabama, 5–8 May 2003, pp. 147–153.
3. Sharma, G., Merry, C. J., Goel, P. and McCord, *Int. J. Remote Sensing*, 2006, **27**, 779–797.
4. Pesaresi, M., Gutjahr, K. H. and Pagot, E., *Int. J. Remote Sensing*, 2008, **29**, 1221–1228.

5. Leitloff, J., Hinz, S. and Stilla, U., *IEEE Trans. Geosci. Remote Sensing*, 2010, **48**, 2795–2806.
6. Jin, X. and Davis, C. H., *Image Vis. Comput.*, 2007, **25**, 1422–1431.
7. Kääb, A., Vehicle velocity from WorldView 2 imagery, 2011; ftp://ccar.colorado.edu/pub/pacificf/DataFusionContest/papers/3.pdf (accessed on 14 July 2012).
8. Salehi, B., Zhang, Y. and Zhong, M., *IEEE J. Select. Top. Appl. Earth Obs. Remote Sensing*, 2012, **5**, 135–145.
9. Updike, T. and Comp, C., DigitalGlobe, Radiometric use of WorldView-2 Imagery, Technical note, 2010; [http://www.digitalglobe.com/downloads/Radiometric\\_Use\\_of\\_WorldView-2\\_Imagery.pdf](http://www.digitalglobe.com/downloads/Radiometric_Use_of_WorldView-2_Imagery.pdf) (accessed on 14 July 2012).
10. DGCA India, <http://dgca.nic.in/reports/air-ind.htm> (accessed on 14 July 2012).
11. ATR 72-500, [http://www.atlanticsunairways.com/training/checklist\\_atr72.pdf](http://www.atlanticsunairways.com/training/checklist_atr72.pdf) (accessed on 14 July 2012).
12. ATR, 2012, <http://www.atraircraft.com/products/atr-72-500.html> (accessed on 14 July 2012).
13. Yan, Gao, P., Sun, H. and Zhao, H., In *Aerospace Technologies Advancements* (ed. Arif, T. T.), InTech, 2010, p. 492.

ACKNOWLEDGEMENTS. We thank DigitalGlobe Inc for providing sample WV 2 imagery. A.G. acknowledges CSIR, New Delhi for funding the research.

Received 14 September 2012; revised accepted 1 May 2013

ANIRUDDHA GHOSH  
P. K. JOSHI\*

TERI University,  
10, Institutional Area,  
Vasant Kunj,  
New Delhi 110 070, India  
\*For correspondence.  
e-mail: pkjoshi27@hotmail.com